Proceedings of the INMM & ESARDA Joint Virtual Annual Meeting
August 23-26 & August 30-September 1, 2021

Scintillator Coupled with Photographic Film for Application to Zero-Knowledge Verification

Jihye Jeon[1], Robert Goldston[1,2], Alexander Glaser[1], Erik Gilson[2]
[1]Program on Science Global and Security, Princeton University, Princeton, NJ, USA
[2]Princeton Plasma Physics Laboratory, Princeton, NJ, USA

ABSTRACT

Verifying the authenticity of nuclear warheads requires gaining confidence on whether an object is a nuclear weapon, without revealing any sensitive information. A zero-knowledge protocol using pre-loadable superheated-emulsion (bubble) detectors has previously been studied for this purpose. As a possible higher-spatial-resolution alternative to bubble detectors, we are studying a detection system based on a ZnS(Ag) scintillator coupled with photographic film. Similar to bubble detectors, photographic film can be pre-loaded prior to an inspection. As a preliminary experiment, two types of ZnS(Ag) scintillators were tested: a 1" diameter Eljen-410 fast neutron detector in a Hornyak button configuration and a 25 cm × 5 cm, 3 mm thick ZnS(Ag), screen manufactured by RC Tritec. A light-tight box containing the scintillator in direct contact with the film was placed 1 m away from a deuterium-tritium (D-T) neutron generator at the Princeton Plasma Physics Laboratory (PPPL). In a series of experiments, the target was exposed to 14 MeV neutrons, covered partially by different shielding materials for image contrast. We could confirm that the image from the Eljen-410 button indicates the presence of shielding material but the embedded light guide complicated quantitative analysis. On the other hand, we could see that the Tritec screen coupled with Ilford HP5+ 400 film works well to discriminate different shielding materials with spatial resolution ~ 3 mm. The proposed method could present another pathway toward a practical and robust system for nuclear warhead verification.

INTRODUCTION

In arms control treaty verification, it is generally deemed important not to reveal sensitive information about the materials or design of nuclear weapons. The host, whose weapons are under inspection, may require high confidence that no information is revealed. On the other hand, an inspector would want to confirm with high confidence whether inspected items are real nuclear warheads. Thus, the verification will be performed with many constraints.

To address these different concerns, we can introduce a cryptographic method to protect information and give confidence in this very low trust situation. In this context, our group previously proposed a zero-knowledge protocol (ZKP) as a template approach [1] and showed that a superheated emulsion or bubble detectors can be used for this purpose. Bubble detectors do not need electronic readout devices, which reduces security concerns, and they can be preloaded prior to a measurement [2]. However, bubble detectors have relatively low efficiency and low

spatial resolution, and the detector response is sensitive to temperature. For this reason, we have been examining alternative methods to improve effectiveness and efficiency of the protocol implementation, a system with a fast neutron scintillator screen close-coupled to commercial photographic film. The most important feature of this system is that we can use it for ZKP verification since we can make a preload on the film and in principle get a flat image if we make another exposure on top of it. In this study, we explored the feasibility of this system for the purpose of our application.

METHODS

We used a collimated neutron source, the Experiment for Calibration with Uranium collimator (the EXCALIBUR) [3], located at the Princeton Plasma Physics Laboratory, PPPL. It consists of a deuterium-tritium neutron generator, which is capable of emitting up to about 3×10^8 14-MeV neutrons per second, surrounded by a carbon steel moderator and borated polyethylene collimator. For this application, we used the EXCALIBUR only in transmission mode, i.e., with an open channel and without any moderation. We used two different detector geometries: an Eljen-410 fast neutron detector with a dimension of 1-inch diameter and 1.6 cm height, in a Hornyak button configuration, and a 25 cm × 5 cm, 3 mm thick ZnS(Ag), screen scintillator manufactured by RC Tritec. The scintillators were kept in the dark for one or two days before the experiment to avoid afterglow effects, or phosphorescence, due to prior light exposure.

Button (EJ-410)

We prepared a 3D-printed light-tight box housing a 1-inch diameter ZnS(Ag) loaded fast neutron scintillator (“button”, EJ-410 from Eljen Technology) in close contact with a 4”×5” sheet of Ilford HP5+ 400 photographic film. This box was exposed to the 14 MeV neutrons from the EXCALIBUR for 10, 20 and 30 minutes at 1 m away from the source. The button was half covered by a 5.5 cm-thick borated polyethylene block as shown in Figure 1.

Screen (Tritec)

We also exposed a 3D-printed light-tight box housing a 25 cm-long, 5 cm-wide, 3 mm-thick ZnS(Ag) loaded screen (from RC Tritec) close-coupled to photographic film to the 14 MeV neutron source. We located the object 1 m away from the source and placed two blocks of stainless steel and lead and three blocks of aluminum in front of the box as shown in Figure 2. All blocks are 2-inch cubes. We exposed each object to neutrons for one hour.

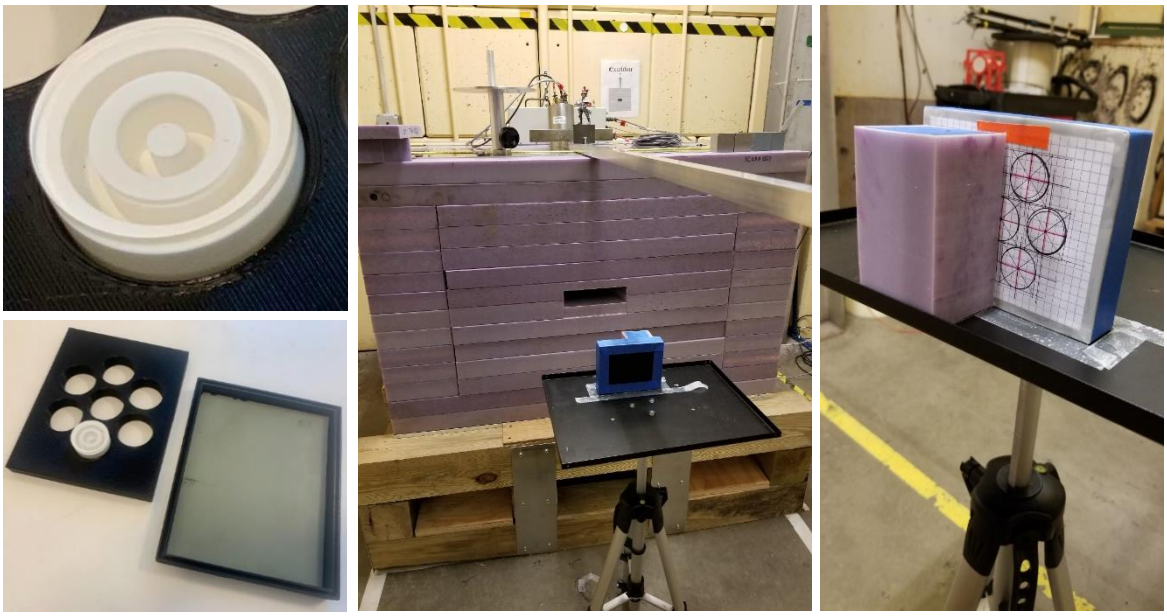

Figure 1. (left, top) A 1" diameter ZnS(Ag) scintillator (EJ-410) and (left, bottom) a 3D-printed light-tight box to hold the scintillator and a 4"×5" photographic film. (middle) A 3D-printed box with the button and a photographic film with a 5.5 cm-thick borated polyethylene (PE) block on a tripot looking into the EXCALIBUR and (right) the PE block in front of the box holding the button and film.

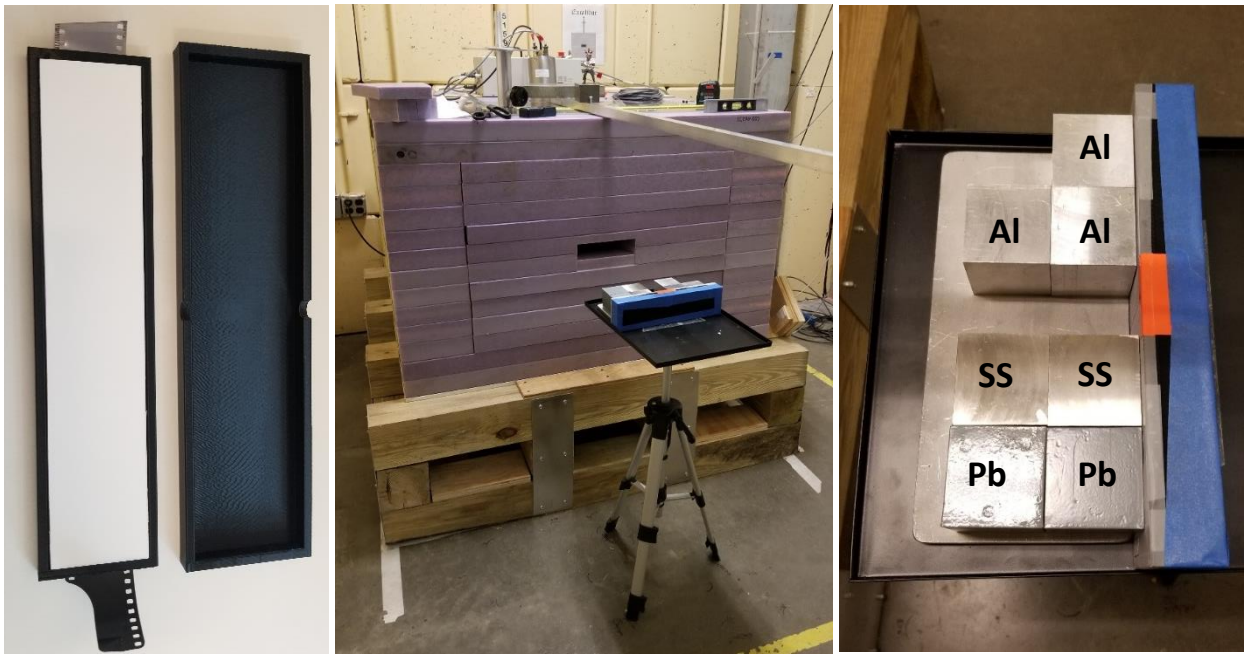

**Figure 2. (left) A 25 cm-long ZnS screen (Tritec) and a 35 mm photographic film in a 3D-printed light-tight box,
(middle) The 3D-printed box with the screen and a photographic film with neutron attenuating blocks on a tripod looking into the EXCALIBUR and
(right) aluminum (Al), stainless steel (SS) and lead (Pb) neutron attenuators in front of the box with the screen and the film.**

For the screen, we modelled the system with MCNP6.2 [4] to better understand the neutron attenuation from different shielding materials. In the model, the 25 cm-wide screen was segmented into 500 cells with a width of 0.5 mm. As shown in Figure 3, the part covered by lead blocks showed more neutrons than the stainless-steel blocks since lead has higher (n,2n) cross sections than iron. From this neutron energy profile, we could see that low-energy neutrons have more curved profile than high energy neutrons.

From this neutron spectrum impinging on the screen, we can calculate the expected optical density on the film by converting neutron fluence to photon fluence and then to image intensity using the characteristic curve of the film [5]. To convert the incoming neutrons to photons emanating from the screen, using detector response curves from the manufacturer may not be appropriate for our application since those curves are acquired using an electronic readout using a photomultiplier tube. In general, fast neutron detector systems use a low-level threshold to discriminate low-amplitude pulses from gamma rays. However, our non-electronic application, just with a photographic film as a readout, does not have that discrimination capability. We therefore need to develop a robust analytic model for scintillation generation from the screen. Fink's semi-quantitative model provides a good starting point, incorporating the neutron interaction with hydrogen, the recoil proton interaction with ZnS, and the photon transmission [6]. Preliminary calculations show that the photon fluence generated from the screen and the optical density on the film had a comparable spatial resolution to high energy neutrons in the energy range of 13–14 MeV. We will further investigate how the lower energy neutrons are generated, even in the region without any shielding material.

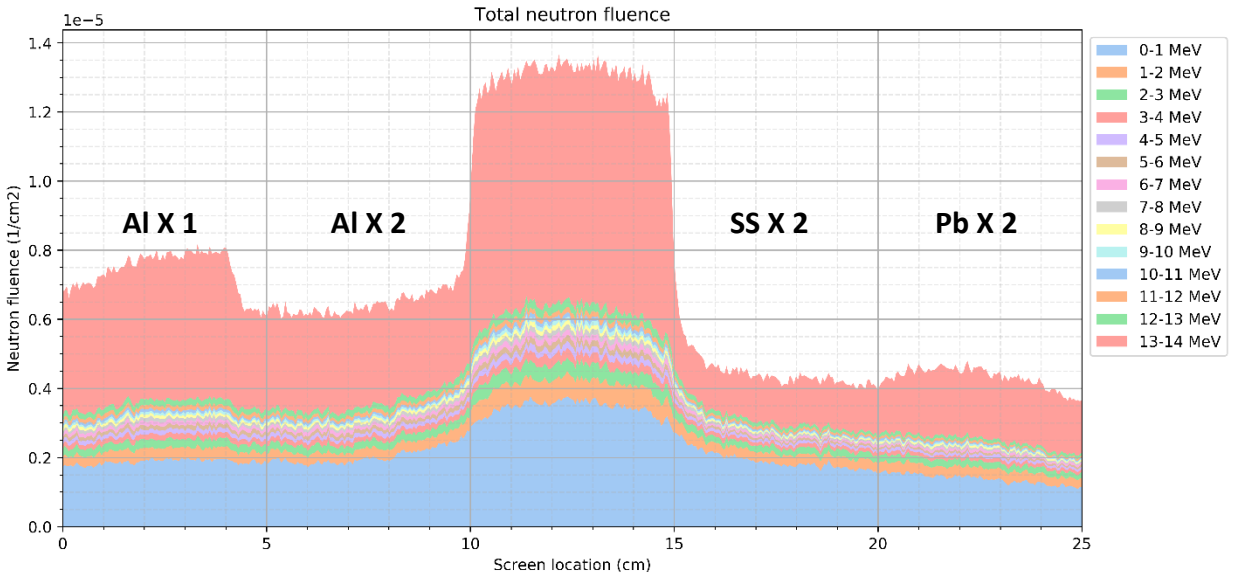

Figure 3. The energy distribution of attenuated neutrons coming into the screen calculated by MCNP6.2.

Film characteristics and analysis

We used only a 4"×5" sheet of Ilford HP5+ 400 photographic film for the button while we tested three kinds of photographic film, 35 mm Ilford HP5+ 400, 35 mm Ilford Delta 3200, a film with high sensitivity, and 35 mm Fujifilm Neopan 100 Acros II, a film with low reciprocity failure under low light conditions. "Low-intensity reciprocity failure" describes an effect where the density of an image produced over a longer period of time is lower when compared to the image with the same total exposure over a shorter period. This is due to the instability of the latent image in its initial stages of formation due to thermal motion [7].

Before the experiment, we pre-exposed the film to enter the linear region of the film's characteristic curve [5], i.e., where the optical density should be linear in the logarithm of the exposure time. The curve consists of three parts: a "toe" region where the density is stagnant with low light exposure, a linear region where the density is proportional to the common logarithm of the light fluence (corresponding to about a 2/3 power), and finally a higher "shoulder" region where the density exhibits a plateau with high exposure. To ensure that we expose neutrons to the screen and the film in the linear regime, we performed a pre-exposure of optical density of ~0.5. For this purpose, we built a customized box containing strips of chips-on-board LEDs to generate a microsecond-range light flash using a pulse/delay generator to pre-expose the film with a uniform image. This pre-exposure gave an optical density of 0.57 on the film.

The exposed films were scanned using an Epson Perfection V850 Pro Photo Scanner. The pixel values were acquired as a 16-bit image and converted to optical density by scanning reference material with an IT8.7/1 standard transparency film with known optical density [8]. Optical density is defined as the negative of the common logarithm of the fraction of light transmitted by the negative. Higher optical density corresponds to greater light absorption in the negative. Since the signal from the button was in a bullseye shape due to the geometry of the scintillator rings and embedded light guide rings, we averaged 200 pixel values, which correspond to 1/3" of the 1" diameter button, in the vertical direction across the center of the button signal for analysis. For the screen analysis, we averaged 280 pixel values, which correspond to 23.7 cm of 35 mm film, in the vertical direction for this analysis.

RESULTS

Button (EJ-410)

The signal from the button showed the geometric pattern as shown in the left figure of Figure 3. The intensity on the film increased with increasing exposure time. We found that the left side of the scintillator, which was covered by the poly block, showed a maximum 0.015 drop in optical density in the right figure of Figure 4, when compared to the uncovered side on the right. This neutron imaging enables us to recognize the existence of neutron attenuating material on the left side of the button. A simple MCNP calculation showed that a 5.5 cm-thick PE block reduces the total neutron fluence to 63.5%, which is not consistent with the relative drop from the right to the left side of the film, as the total signal shows a maximum change in optical density due to exposure of about 0.03. However, the geometry of the button complicates further quantitative analysis since

the scintillation generated from the uncovered side can be evenly spread out within the acrylic rings of the light guide, and this reduces the difference in the signal intensity between the covered and uncovered side.

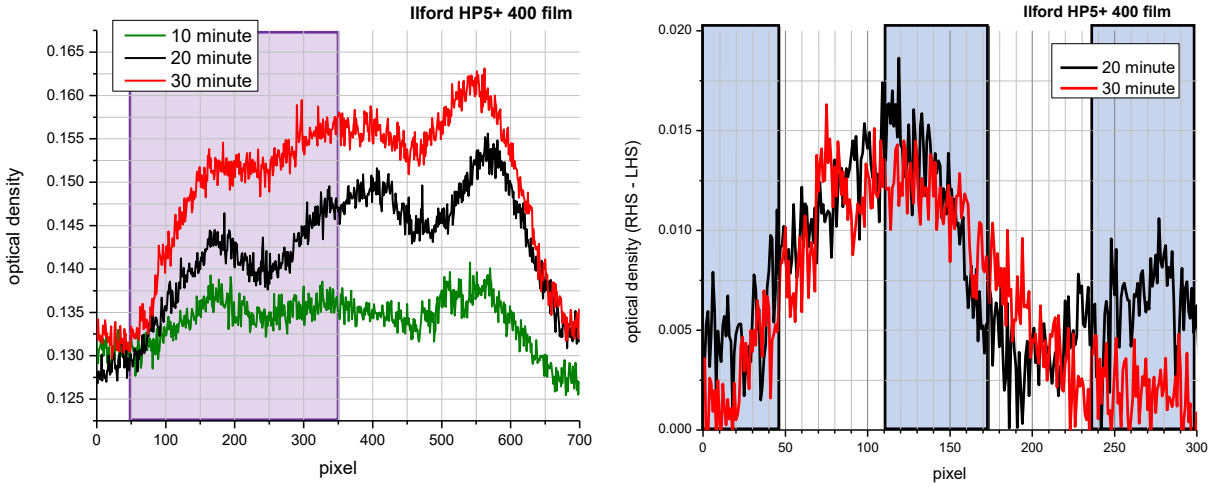

Figure 4. (left) The optical density of the negative film for 10, 20 and 30 minute-exposures of the button. The shaded region over 50-350 pixel is where the PE block was located and the button was placed over 50-650 pixel (600 dpi).
(right) The difference between optical density of the right-hand side and left-hand side of the signal. The shaded regions show where the rings of ZnS(Ag) are located and the unshaded regions are for the rings of light guide.

Screen (Tritec)

From the HP5+ 400 curve in Figure 5, we can see that neutrons are generally attenuated as expected in the different regions: a higher optical density in the region of two aluminum blocks than in the region of two stainless-steel blocks means a darker image on the film, and it implies that the part of the film behind the aluminum saw more scintillation than the part behind the stainless steel. This sharp rise and fall at the edges where the two aluminum blocks and two stainless-steel blocks were adjacent to a region of no attenuation, tells us that the spatial resolution of the screen is on the order of 4 mm or less.

When we exposed neutrons to the screen with different kinds of film, Ilford HP5+ 400 film showed the best contrast in signals due to different shielding materials as shown in Figure 4. The average difference in optical density between the region covered by two aluminum blocks and the unshielded region in the center was 0.057 for HP5+400, 0.025 for Delta 3200 and 0.013 for Acros II 100 film. The average optical density difference between two SS and the unshielded was 0.062 for HP5+ 400, 0.029 for Delta 3200 and 0.015 for Acros II 100. Note that the optical density of unexposed film, due to fog and attenuation in the substrate, was in the range of 0.295–0.310 for HP5+ 400, 0.255–0.270 for Delta 3200 and 0.285–0.295 for Acros II 100 film. We conclude that film with high sensitivity or low reciprocity failure does not enhance the quality of the signals.

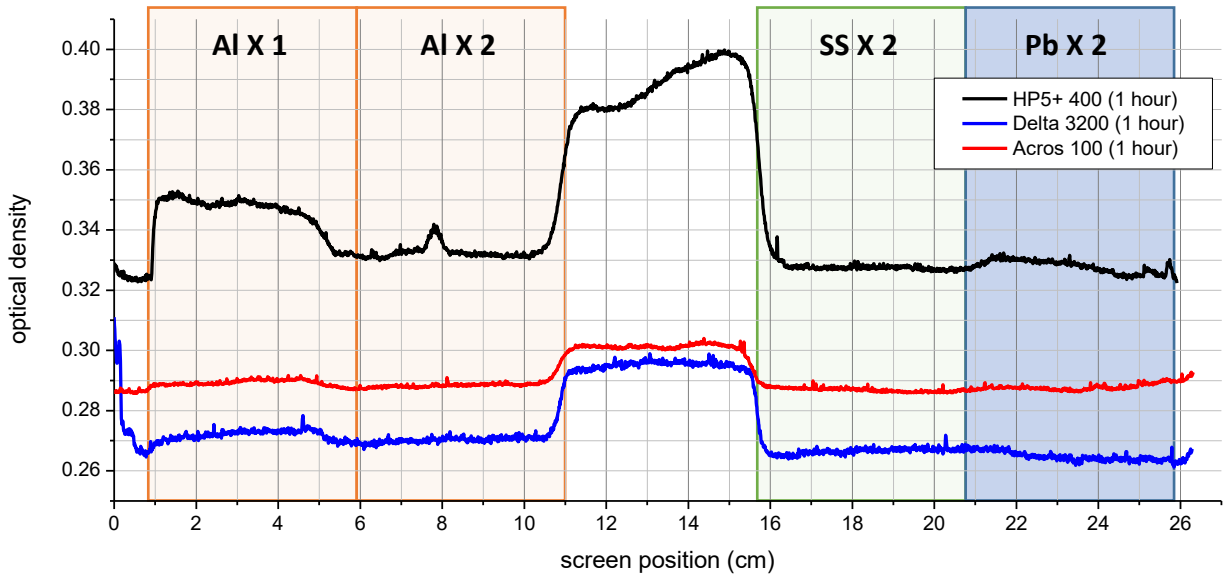

Figure 5. Signals on Ilford HP5+ 400, Ilford Delta 3200 and Fujifilm Neopan Acros II 100 after one hour exposure of 14 MeV neutrons to the film covered with the screen and different shielding materials.

The values of optical density in Figure 5 are located in the "toe" region of the film characteristic curve [5]. As shown in Figure 6, the film with pre-exposure showed more contrast, average optical density difference of 0.057 in the Al region and 0.062 in the SS region when compared to the film without pre-exposure, –0.008 in the Al region and 0.09 in the SS region. Except that the intensity in the uncovered region was lower than that in one and two aluminum regions, the pre-exposed film has greater difference in the average optical density between covered regions than the film without pre-exposure. The average optical density difference between the one Al–two Al region, two Al–two SS region and two SS–two Pb region is 0.0315, 0.0980 and 0.0462 for the pre-exposed film while 0.0144, 0.0055 and 0.0004 for the film without pre-exposure. Therefore, we can assume that pre-exposing films help intensify the signals. We are currently examining why there was more light in the aluminum regions than in the unshielded region.

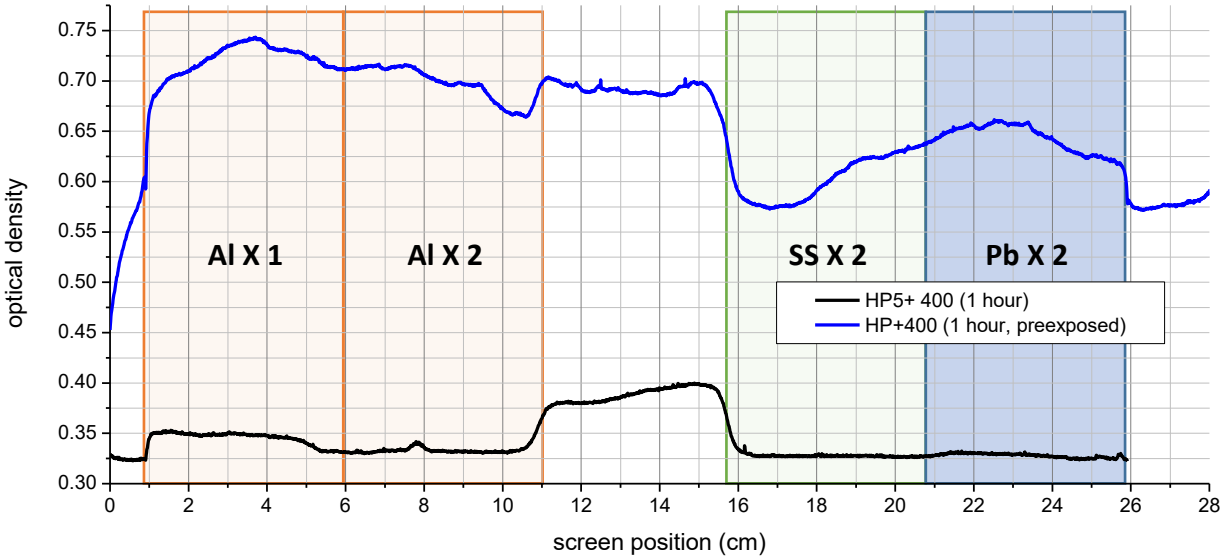

Figure 6. Signals on Ilford HP5+ 400 with and without pre-expsure after one hour exposure of 14 MeV neutrons to the film covered with the screen and different shielding materials.

The difference in total neutron fluence for all neutron energies due to shielding materials shown in Figure 5 and 6 was less distinctive than that from the calculation in Figure 3.

CONCLUSIONS

A ZnS(Ag) fast neutron scintillator coupled with photographic film is a promising option for zero-knowledge protocol verification. This system can perform neutron imaging like bubble detectors with 14 MeV neutrons transmitted through the target, but with higher spatial resolution. Images from a "Hornyak" button showed promising sensitivity, but the embedded light-guide made quantitative analysis complicated. On the other hand, we could see that the Tritec screen coupled with Ilford HP5+ 400 film can discern different materials with a high spatial resolution < 4 mm. We will try to reduce the fluctuation in the film response in the future so that we can acquire more uniform and consistent images for our system to be robust and reliable. Ongoing efforts on developing analytic model for calculating image intensity will enable us to further optimize our system for best imaging results.

ACKNOWLEDGEMENTS

This work was supported by the U.S. Department of Energy under contract number DE-AC02-09CH11466. The United States Government retains a non-exclusive, paid-up, irrevocable, world-wide license to publish or reproduce the published form of this manuscript, or allow others to do so, for United States Government purposes. This work is also supported by the U.S. Department of Energy, National Nuclear Security Administration, Office of Defense Nuclear

Nonproliferation Research and Development. The authors would like to thank Andrew Carpe and Robert Hitchner from PPPL for their technical support to this study.

REFERENCES

[1] Glaser, A., Barak, B. & Goldston, R. A zero-knowledge protocol for nuclear warhead verification. *Nature* 510, 497–502 (2014).

[2] Philippe, S., Goldston, R., Glaser, A. et al. A physical zero-knowledge object-comparison system for nuclear warhead verification. *Nature Communications* 7, 12890 (2016).

[3] Hepler, M., Zero-knowledge Isotopic Discrimination for Nuclear Warhead Verification, PhD dissertations (2020).

[4] Werner, C.J., et al., "MCNP6.2 Release Notes", Los Alamos National Laboratory, report LA-UR-18-20808 (2018).

[5] Ilford Photo (Harman technology Limited), “HP5 Plus Technical Information”, (2018) (available at: https://www.ilfordphoto.com/amfile/file/download/file/1903/product/695/)

[6] Fink, C.L., Optimization of a Hornyak-buton Detector for Fast-neutron Detection, IEEE Transactions on Nuclear Science, Vol. 29, Issue 1, 718-721 (1982).

[7] Webb, J.H., Low Intensity Reciprocity-Law Failure in Photographic Exposure: Energy Depth of Electron Traps in Latent-Image Formation; Number of Quanta Required to Form the Stble Sublatent Image, Journal of the Optical Society of America, Vol. 40, No. 1, 3-13 (1959).

[8] Green, C., Quantitative Densitometry with the Umax Flatbed Scanner – Analysis, University of Illinois, website posted in June 1998 (available at: https://calendar.itg.beckman.illinois.edu/archives/technical_reports/98-004/analysis.htm)